

What Goes beyond Multi-modal Fusion in One-stage Referring Expression Comprehension: An Empirical Study

Gen Luo, Yiyi Zhou*, Jiamu Sun, Shubin Huang, Xiaoshuai Sun, *Member, IEEE*, Qixiang Ye *Senior Member, IEEE*, Yongjian Wu, Rongrong Ji, *Senior Member, IEEE*

Abstract—Most of the existing work in one-stage referring expression comprehension (REC) mainly focuses on multi-modal fusion and reasoning, while the influence of other factors in this task lacks in-depth exploration. To fill this gap, we conduct an empirical study in this paper. Concretely, we first build a very simple REC network called SimREC, and ablate 42 candidate designs/settings, which covers the entire process of one-stage REC from network design to model training. Afterwards, we conduct over 100 experimental trials on three benchmark datasets of REC. The extensive experimental results not only show the key factors that affect REC performance in addition to multi-modal fusion, e.g., multi-scale features and data augmentation, but also yield some findings that run counter to conventional understanding. For example, as a vision and language (V&L) task, REC does is less impacted by language prior. In addition, with a proper combination of these findings, we can improve the performance of SimREC by a large margin, e.g., +27.12% on RefCOCO+, which outperforms all existing REC methods. But the most encouraging finding is that with much less training overhead and parameters, SimREC can still achieve better performance than a set of large-scale pre-trained models, e.g., UNITER and VILLA, portraying the special role of REC in existing V&L research¹.

I. INTRODUCTION

Referring expression comprehension [1]–[5], also known as *visual grounding* [6]–[9] or *phase grounding* [10]–[12], is a task of locating the target instance in an image based on the natural language expression. Compared with the traditional object detection task [13], [14], REC is not limited to a fixed set of object categories and can theoretically perform any open-ended detection according to the text description [15]. These appealing properties enable REC to garner widespread attention from the communities of both computer vision (CV) and vision and language (V&L) [1], [2], [2]–[5], [10]–[12].

Due to the obvious advantage in efficiency, one-stage modeling has recently become the main research focus in REC [1],

G. Luo, Y. Zhou, J. Sun, S. Huang, X. Sun and R. Ji are with the Media Analytics and Computing Lab, Department of Artificial Intelligence, Xiamen University, China (e-mail: luogen@stu.xmu.edu.cn, zhouyiyi@xmu.edu.cn, sunjiamu@stu.xmu.edu.cn, shubinhuang@stu.xmu.edu.cn, xs-sun@xmu.edu.cn, rrji@xmu.edu.cn).

Q. Ye is with the Peng Cheng Laboratory, Shenzhen 518066, China, and also with the School of Electronics, Electrical and Communication Engineering, University of Chinese Academy of Sciences, Beijing 100049, China (e-mail: qxye@ucas.ac.cn).

Y. Wu is with the Tencent Technology (Shanghai) Co., Ltd, China (e-mail: littlenwu@tencent.com).

*Corresponding Author: Yiyi Zhou (E-mail: zhouyiyi@xmu.edu.cn)

¹Source codes will be released: <https://github.com/luogen1996/SimREC>.

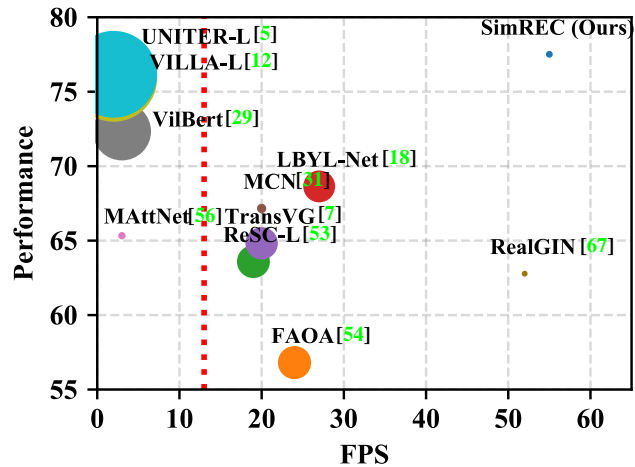


Fig. 1: Comparison of performance and inference speed between SimREC and other REC methods on the *val* set of RefCOCO+ [19]. The point size corresponds to the number of parameters. FPS denotes frames per second. The points to the left side of the red line are two-stage methods, while the rest are one-stage. By combing the findings of the empirical study, SimREC greatly outperforms all existing REC methods.

[2], [7]–[9]. Compared with the two-stage methods [3], [5], [6], [10], [17], one-stage models can omit the generation of region proposals and directly output the bounding box of the referent without complex image-text ranking, thereby improving the inference speed by an order of magnitude, as shown in Fig. 1. However, one-stage models often have worse performance than the two-stage ones [1], [2], [7]. Practitioners mainly attribute this shortcoming to the lack of enough multi-modal reasoning ability [1], [8], [9], [18]. To this end, recent endeavors put numerous efforts into the design of the multi-modal fusion branch of one-stage REC, which have achieved notable success [1], [8], [9], [18].

Despite these advances, the existing literature still lacks a comprehensive study to gain insight into one-stage REC. Differing from other V&L tasks, one-stage REC not only needs to realize the joint understanding of two modalities, but also requires very accurate language-vision alignments, *i.e.*, detection. Therefore, in addition to multi-modal fusion, other important factors, such as visual backbone, detection head and training paradigm, also need to be explored in depth. In this

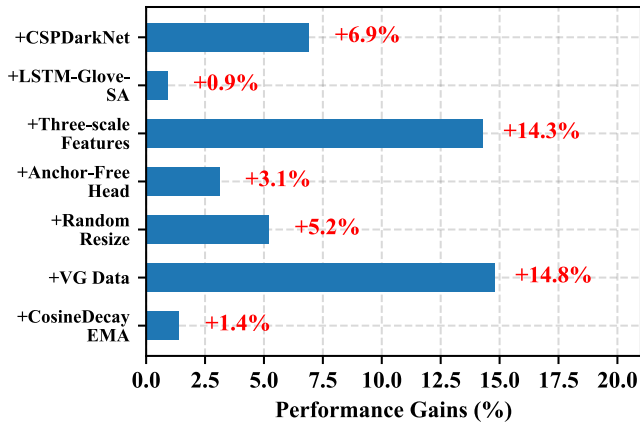


Fig. 2: Statistical results of the impact of components in one-stage REC on the *val* set of RefCOCO+.

paper, we are committed to filling this research gap. We aim to figure out *what also matter in one-stage REC*, and *how they affect the REC performance*. Meanwhile, we also hope to verify that as an V&L task, *whether REC can be a survivor in the era dominated by large-scale BERT-style pre-trained models* [16], [20]–[22].

To approach these targets, we first build a very simple one-stage REC network called *SimREC*, of which structure is given in Fig. 3. Based on this network, we conduct an empirical research that ablates 42 candidate designs / settings, which cover the most components of one-stage REC, such as visual backbone, language encoder, detection head and training paradigm *et al.* Afterwards, we conduct over 100 experimental trials on three benchmark datasets, namely RefCOCO [19], RefCOCO+ [19] and RefCOCOG [23], to examine the effects of these candidates. Lastly, these results constitute the main analysis data of this research.

This study yields significant findings for one-stage REC. Above all, it identifies the key factors that affect performance. As shown in Fig. 2, visual backbone and multi-scale visual features are important for performance improvement. And data augmentation, including image augmentation methods [24]–[27] and additional data [28], is also very beneficial. Meanwhile, we obtain some findings against the conventional impressions about REC. For example, REC is less affected by language modeling, which is however very essential in other V&L tasks like visual question answering [29]–[32]. In addition, we also notice that although some candidate designs obtain the expected performance gains, their practical use is still different to that in other tasks, *e.g.*, augmentation methods [24]–[27]. Detailed discussions are given in the experimental section.

By adopting these empirical findings, we improve the performance of our baseline network *SimREC* by a large margin, *e.g.*, from 50.39 to 77.51 on RefCOCO+. Thus, this simple network can greatly outperform all existing one-stage and two-stage methods in both accuracy and inference speed, as shown in Fig. 1. More importantly, with less training overhead and parameters, *SimREC* can achieve better performance than a

bunch of large-scale pre-trained models [16], [20]–[22], *e.g.*, VILLA-Large [21], on all benchmark datasets. We believe this result can be very enlightening for the existing V&L research, where the most tasks are dominated by the expensive large-scale models.

II. RELATED WORK

Referring Expression Comprehension (REC) [1], [2], [5], [8], [33]–[40] is a task to locate the target referent based on a natural language expression. Early works [5], [33]–[41] of REC often follow a two-stage pipeline. Concretely, these two-stage models first detect the salient regions of a given image as candidate instances by a pre-trained detection network, *e.g.*, Faster-RCNN [42]. Afterwards, the multi-modal matching module is deployed for measuring the similarities of region-expression pairs, based on which the most matching one is selected as the prediction result. Besides, addition modules for learning features of relationships and locations can be also plugged into the pipeline to enhance the reasoning ability [3]. This paradigm achieves great success in the early development of REC [5], [39]–[41], but they also have obvious defects in model efficiency and generalization [7], [43].

To this end, one-stage REC has recently become a popular research direction [1], [2], [4], [7], [8], [18], [43]. Specifically, one-stage REC models regard the task as a multi-modal regression problem and directly output the predicted boxes of referents. By omitting the steps of region detection and image-text matching in multi-stage modeling, one-stage models greatly speed up the inference time, *e.g.*, 28.6 images per second, as reported in [1]. However, one-stage models often have worse REC performance compared with the two-stage methods, like *MattNet* [3], mainly due to the limited reasoning ability. In this case, recent advances put efforts to improve the reasoning ability of one-stage REC and propose various novel multi-modal networks for one-stage REC [1], [8], [9], [18]. In this paper, except the well studied multi-modal fusion, we focus on the examination of other components in one-stage REC, which still lacks a systematic study.

With the recent prevalence of large-scale V&L pre-training, the new SOTA performance of REC is also inevitably obtained by these large-scale pre-training models [16], [20]–[22], [44]. Specifically, these models are pre-trained with millions of image-text examples and large-scale parameters, thereby obtaining superior vision-language alignment ability. On REC, most of these models follow the two-stage paradigm and regard this task as a text and image region matching problem [16], [20]–[22]. In this paper, we want to find out whether a well studied one-stage model can be better than these expensive pre-trained models.

III. SIMREC

To accomplish the empirical study, we first build a very simple one-stage REC network called *SimREC*, of which structure is given in Fig. 3. Based on *SimREC*, we prepare a set of candidate designs and settings to examine the impact of different components.

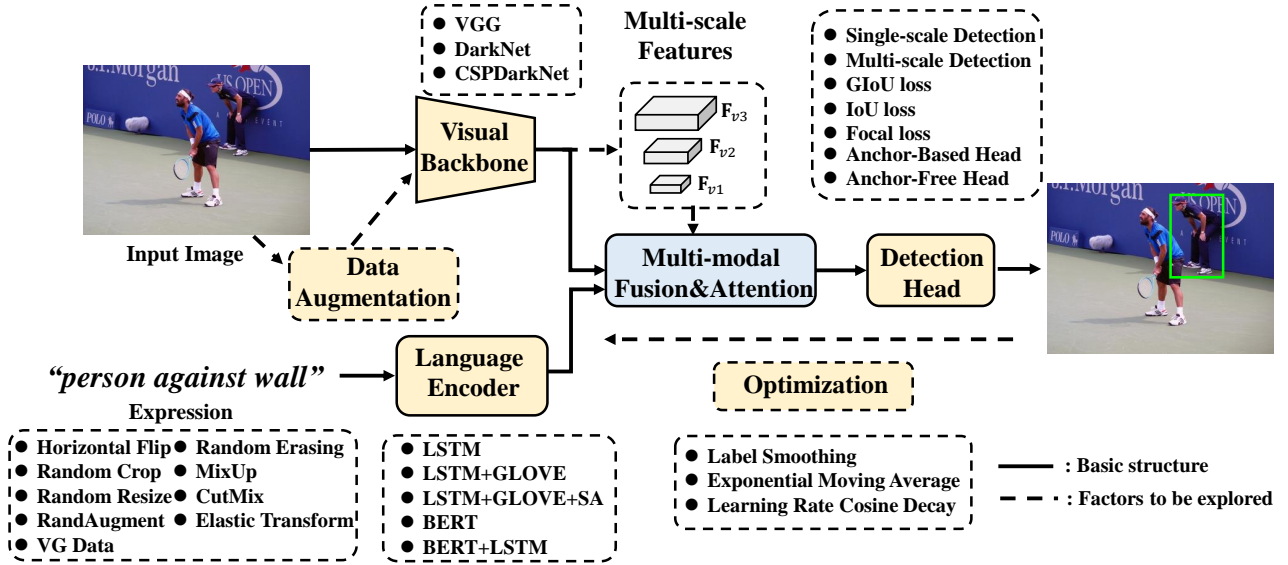


Fig. 3: The framework of the proposed SimREC. The solid lines depict the basic structure of SimREC. It includes a visual backbone and a language encoder to extract features of two modalities, respectively, based on which two simple modules are deployed for multi-modal fusion and reasoning. Afterwards, a detection head is used to predict the bounding box of the referent. The dashed parts list candidate designs for the empirical study, which are used to examine the effects of different components in one-stage REC.

A. Basic Structure

Given an image I and an expression E , SimREC uses a visual backbone and a language encoder to extract the visual and text features, denoted as $\mathbf{F}_v \in \mathbb{R}^{h \times w \times d}$ and $\mathbf{F}_t \in \mathbb{R}^{l \times d}$, respectively. Here, $h \times w$ denotes the resolution of visual feature maps, and l is the length of the expression. Then, the text features \mathbf{F}_t are attentively pooled [29] to a global vector $f_t \in \mathbb{R}^d$. Afterwards, a simple multi-modal fusion module is deployed to obtain the joint representations of two modalities, denoted as $\mathbf{F}_m \in \mathbb{R}^{h \times w \times d}$, which is obtained by:

$$f_m = \sigma(f_v \mathbf{W}_v) \odot \sigma(f_t \mathbf{W}_t). \quad (1)$$

Here, f_m and f_v are the feature vectors of \mathbf{F}_m and \mathbf{F}_v , respectively, and σ denotes the ReLU [45] activation function. To keep a certain reasoning ability, we also apply an attention unit called GARAN [1] after the multi-modal fusion.

Lastly, a regression layer is deployed to predict the bounding box of the referent in the image. Specifically, for each grid (g_x, g_y) , SimREC predicts raw coordinates of the bounding box $\{t_x, t_y, t_w, t_h\}$ and its corresponding confidence score c . Afterwards, the final bounding box $b = \{b_x, b_y, b_w, b_h\}$ is calculated based on the pre-defined anchor box (p_w, p_h) by

$$\begin{aligned} b_x &= \text{sigmoid}(t_x) + g_x, \\ b_y &= \text{sigmoid}(t_y) + g_y, \\ b_w &= p_w^{e^{t_w}}, b_h = p_h^{e^{t_h}}. \end{aligned} \quad (2)$$

Given the ground-truth box $b' = \{b'_x, b'_y, b'_w, b'_h\}$ and the ground-truth confidence c' , the loss function of SimREC is defined as:

$$l(b_i, b'_i, c_i, c'_i) = \sum_{i=1}^{h \times w \times n} c'_i * l_{box}(b'_i, b_i) + l_{conf}(c'_i, c_i) \quad (3)$$

Here, n is the number of pre-defined anchor boxes. l_{box} and l_{conf} denote the regression loss and the binary prediction loss of the confidence score, respectively. During the test stage, SimREC will select the bounding box with the highest confidence score as the final prediction.

B. Candidate Designs

Visual Backbone. SimREC uses DarkNet [46] as the default visual backbone. VGG [47] and the recently proposed CSPDarkNet [48] are the candidate choices. Meanwhile, we also test the effects of different image resolutions.

Language Encoder. The default language model for SimREC is an LSTM network [49] with GLOVE embeddings [50]. During experiments, we will enhance the ability of language encoder by adding advance designs like self-attention [51] and BERT embedding [52].

Multi-scale Features and Detection. We also experiment SimREC with multi-scale features and multi-scale detection setting. In terms of multi-scale features, we use the last k scale feature maps of the visual backbone as our visual features, denoted as $\{\mathbf{F}_{vi}\}_{i=1}^k$. The features of each scale are fused with the text ones by the multi-scale fusion scheme proposed in [2], denoted as $\{\mathbf{F}_{mi}\}_{i=1}^k$. Only the last scale feature maps are used, *i.e.*, \mathbf{F}_{mk} . In terms of multi-scale detection, each scale feature in $\{\mathbf{F}_{mi}\}_{i=1}^k$ will use a corresponding detection head to predict bounding boxes.

Detection Paradigms. In addition to the anchor-based detection head [46], we also apply the recently popular anchor-free detection [53] to SimREC. Specifically, in REC, the anchor-free detection removes the dependency of pre-defined

anchors, thus the predictions of the width b_w and height b_h in Eq 2 will be modified to:

$$b_w = e^{t_w}, b_h = e^{t_h}. \quad (4)$$

We also try different loss functions, including *IoU* loss [54], *GIoU* loss [54], *Smooth-L1* loss [42] and *Focal* loss [55].

Data Augmentation. We adopt additional data, *i.e.*, Visual Genome [28], and image augmentation methods [24]–[27], [56] for data augmentation. In terms of image augmentation, we try the common ones in object detection [42], [46] including *Horizontal Flip*, *Random Erasing* [24], *Elastic-Transform*, *CutMix* [26], *Random Resize*, *RandAugment* [25] and *MixUp* [56]. We make some modifications to ensure them applicable to one-stage REC, *e.g.*, we remove the color inversion and the cutout [27] from the augmentation pool of RandAugment [25], and abandon the mixing objectives of MixUp [56].

Optimizations. To regularize and accelerate the model training, we also examine some training techniques, *e.g.*, label smoothing [57], exponential moving average (EMA) [58] and cosine decay learning schedule [57].

IV. EXPERIMENTS

A. Datasets and Metric

RefCOCO & RefCOCO+ [19] contain 142k referring expressions for 50k bounding boxes in 19k images from MS-COCO [13]. There are four splits in RefCOCO and RefCOCO+, *i.e.*, *train*, *val*, *testA* and *testB*, with a number of 12k, 10k, 5k, 5k images, respectively. Test A contains more *people* instances, while Test B has more *object* ones. The expressions of RefCOCO are mainly about absolute spatial relationships, while the ones of RefCOCO+ are about attributes and relative relations. **RefCOCOg** [23], [59] has 104k expressions for 54k objects from 26k images. It has two different partitions, *i.e.*, *Google* split [59] and *UMD* split [23]. Google split only contains training set and validation set, and images of which are overlapped. Instead, *UMD* split avoids overlapping partitions, and it contains three splits, *i.e.*, *train*, *validation* and *test*. In particular, the expressions of RefCOCOg are longer and more complex than those of RefCOCO and RefCOCO+. **Visual Genome** [28] contains 5.6M referring expressions for 101K images. Compared to RefCOCO, RefCOCO+ and RefCOCOg, the expressions of Visual Genome are more diverse but their annotations are relatively noisy.

Intersection-over-Union (IoU) is the metric used in REC, which measures the overlap degree between the prediction and the ground-truth. Following previous works [1], [2], [7], [8], we use *IoU@0.5* to measure prediction accuracy.

B. Experimental Settings

Network Configurations. The visual backbone and the language encoder of SimREC are a CSPDarknet [48] and an LSTM [49] with a self-attention layer [51], respectively. For SimREC, we use three-scale visual features from the visual backbone outputs of stride=8, stride=16 and stride=32, of which dimensions are 256, 512, 1024, respectively. For

language encoder, its dimension is set to 512 and the word embedding is a 300-d matrix initialized by pre-trained glove vectors [50]. By default, the input image is resized to 416×416 , and the maximum length of input expressions is set to 15 for RefCOCO and RefCOCO+, and 20 for RefCOCOg. For detection head and loss function, we apply the anchor-free head [53] with IoU loss [54] and BCE loss. For data augmentations, random resize is used in the training. To improve the training efficiency, we further apply the exponential moving average (EMA) [58] and cosine decay learning schedule.

Training settings. We use Adam [62] to train our models for 40 epochs, which can be reduced to 25 epochs when EMA is applied. The learning rate is initialized with $1e-4$ and will be decayed by 10 at the 35-th, 37-th and 39-th epoch, respectively. We also try the cosine decay as the learning rate schedule. All visual backbones are pre-trained on MS-COCO [13], while the images appeared in the val and test sets of three REC datasets are removed. We also apply the region annotations in the Visual Genome [63] to pre-train SimREC. Particularly, pre-trained stage takes 15 epochs with a batch size of 256. The learning rate and optimization are kept the default settings.

C. Experimental Results

1) Ablation Study: We first conduct extensive experiments on benchmark datasets to ablate the candidate designs/settings described in Sec. IV-C1, of which results are shown in Tab. I. **What matters in one-stage REC?** From Tab. I, we first observe that the visual components are critical for one-stage REC. The use of a better backbone or detection head can lead to significant performance gains, *e.g.*, up to +6.3% and +3.1% on RefCOCO+, respectively. Meanwhile, larger image resolutions are also more beneficial for performance. These results are within the scope of existing CV and V&L studies [42], [46], [64]–[66].

Multi-scale visual features are the factor that can boost performance. On RefCOCO+, its performance gain can reach up to +14.3%, while the ones on the other two datasets are also about +6%. However, when combining it with multi-scale detection, the performance is not further improved. This result suggests that multi-scale features are basically used to enhance the descriptive power of visual backbones rather than multi-scale detection, which is obviously different to the use in object detection [42], [46].

Data augmentation is another factor that greatly affects performance. Using Visual Genome (VG) as the additional training data can greatly boost performance on all benchmarks. Meanwhile, a simple image augmentation like *Resizing* also obtain obvious performance gains. These results suggest that one-stage REC has a great demand in training data, especially compared with other V&L tasks [31], [32]. For example, VG is often used as additional data in VQA, while the improvement is often marginal [29], [67]. From Tab. I, we can also summarize a prerequisite for data augmentation, which is that the semantics of image-text pairs should not be damaged. The operations like *Horizontal Flip* and *Random Crop* will reduce the completeness or the correctness of REC examples, thus leading to counterproductive results. Meanwhile, strong

TABLE I: Ablation studies of different factors on three REC datasets. † denotes the settings of the basic structure and ‡ denotes the settings of SimREC. For all the results, we average three experimental results of different random seeds.

Factors	Choices	RefCOCO val		RefCOCO+ val		RefCOCOg val		Inference Speed ²		Training Time	
		Acc	Δ	Acc	Δ	Acc	Δ	FPS	Δ	Hours	Δ
Visual Backbone	DarkNet-53†	70.63	+0.00	50.39	+0.00	58.78	+0.00	59.2	+0.0	6.6 h	+0.0h
	VGG-16	70.12	-0.51	49.81	-0.58	58.22	-0.56	46.9	-12.3	9.9 h	+3.3h
	CSPDarkNet-53‡	71.90	+1.17	57.24	+6.85	57.58	-1.20	74.1	+14.9	5.4 h	-1.2h
Language Encoder	LSTM+GLOVE†	70.63	+0.00	50.39	+0.00	58.78	+0.00	59.2	+0.0	6.6 h	+0.0h
	LSTM	70.06	-0.57	49.54	-0.85	57.78	-1.00	59.2	+0.0	6.6 h	+0.0h
	LSTM+GLOVE+SA(1)‡	71.56	+0.93	51.26	+0.87	58.11	-0.67	58.1	-1.1	6.7 h	+0.1h
	LSTM+GLOVE+SA(2)	71.17	+0.54	50.65	+0.26	58.42	-0.36	57.1	-2.1	6.7 h	+0.1h
	LSTM+GLOVE+SA(3)	71.43	+0.80	48.73	-1.66	59.15	+0.37	55.9	-3.3	6.7 h	+0.1h
	LSTM+BERT	70.66	+0.03	50.27	-0.12	60.31	+1.53	42.0	-17.2	7.8 h	+1.2h
Multi-scale Features	One-scale Feature†	70.63	+0.00	50.39	+0.00	58.78	+0.00	59.2	+0.0	6.6 h	+0.0h
	Two-scale Features	76.79	+6.16	63.71	+13.32	62.62	+3.84	54.1	-5.1	7.9 h	+1.3h
	Three-scale Features‡	77.41	+6.78	64.72	+14.33	65.51	+6.73	49.0	-10.2	10.8 h	+4.2h
	Four-scale Features	78.33	+7.70	65.21	+14.82	65.56	+6.78	42.9	-16.3	11.1 h	+4.5h
Multi-scale Detection	One-scale Feature+Head $\times 1$ †	70.63	+0.00	50.39	+0.00	58.78	+0.00	59.2	+0.0	6.6 h	+0.0h
	Three-scale Features+Head $\times 1$ ‡	77.41	+6.78	64.72	+14.33	65.51	+6.73	49.0	-10.2	10.8 h	+4.2h
	Three-scale Features+Head $\times 3$	77.40	+6.77	62.78	+12.39	64.73	+5.95	39.2	-20.0	14.5 h	+7.9h
Detection Head	Anchor-Based†	70.63	+0.00	50.39	+0.00	58.78	+0.00	59.2	+0.0	6.6 h	+0.0h
	Anchor-Free‡	73.65	+3.02	53.49	+3.10	59.46	+0.68	55.9	-3.3	9.1 h	+2.5h
Loss Fuction	BCE+MSE†	70.63	+0.00	50.39	+0.00	58.78	+0.00	59.2	+0.0	6.6 h	+0.0h
	Focal loss+MSE	70.43	-0.20	49.86	-0.53	58.42	-0.36	59.2	+0.0	6.7 h	+0.1h
	BCE+SmoothL1	71.12	+0.49	50.29	-0.10	59.23	+0.45	59.2	+0.0	6.7 h	+0.1h
	BCE+IoU loss‡	71.39	+0.76	51.68	+1.29	59.54	+0.76	59.2	+0.0	6.7 h	+0.1h
	BCE+GIoU loss	70.76	+0.13	50.34	-0.05	59.42	+0.64	59.2	+0.0	6.7 h	+0.1h
Input Resolution	416×416 † ‡	70.63	+0.00	50.39	+0.00	58.78	+0.00	59.2	+0.0	6.6 h	+0.0h
	256×256	64.57	-6.06	47.25	-3.14	52.63	-6.15	69.0	+9.8	3.6 h	-3.0h
	320×320	68.53	-2.10	49.13	-1.26	56.86	-1.92	67.1	+7.9	5.0 h	-1.6h
	512×512	70.97	+0.34	51.28	+0.89	59.97	+1.19	46.9	-12.3	9.6 h	+3.0h
	608×608	71.15	+0.52	51.59	+1.20	59.38	+0.60	41.0	-18.2	12.6 h	+6.0h
Data Augmentations	None†	70.63	+0.00	50.39	+0.00	58.78	+0.00	59.2	+0.0	6.6 h	+0.0h
	Horizontal Flip	66.58	-4.05	47.92	-2.47	56.13	-2.65	59.2	+0.0	6.6 h	+0.0h
	Random Crop	61.20	-9.43	47.06	-3.33	51.67	-7.11	59.2	+0.0	6.8 h	+0.2h
	Elastic Transform	71.91	+1.28	52.36	+1.97	60.58	+1.80	59.2	+0.0	6.7 h	+0.1h
	Random Resize‡	74.07	+3.44	55.61	+5.22	62.79	+4.01	59.2	+0.0	7.8 h	+1.2h
	RandAugment	72.89	+2.26	53.23	+2.84	61.85	+3.07	59.2	+0.0	7.6 h	+1.0h
	Random Erasing	71.29	+0.66	51.79	+1.40	59.62	+0.84	59.2	+0.0	7.4 h	+0.8h
	Mixup	72.63	+2.00	51.09	+0.70	59.56	+0.78	59.2	+0.0	7.2 h	+0.6h
	CutMix	72.42	+1.79	52.40	+2.01	60.42	+1.64	59.2	+0.0	7.2 h	+0.6h
	VG Data‡	78.23	+7.60	65.18	+14.79	70.40	+11.62	59.2	+0.0	118.3h	+111.7h
Optimizations	None†	70.63	+0.00	50.39	+0.00	58.78	+0.00	59.2	+0.0	6.6 h	+0.0h
	Label Smoothing	70.78	+0.15	50.93	+0.54	59.27	+0.49	59.2	+0.0	6.6 h	+0.0h
	Exponential Moving Average‡	71.95	+1.32	51.78	+1.39	60.46	+1.68	59.2	+0.0	5.1 h	-1.5h
	Learning Rate Cosine Decay‡	70.79	+0.16	50.63	+0.30	59.44	+0.66	59.2	+0.0	6.6 h	+0.0h

TABLE II: Performance of combining different data augmentations.

Data Augmentations	RefCOCO (val)	
	Acc	Δ
Random Resize (Baseline)	74.07	+0.00
MixUp+CutMix	72.61	-1.46
RandAugment+Elastic Transform	71.99	-2.08
RandAugment+Random Resize	73.77	-1.00
MixUp+Random Resize	71.51	-2.56
All Useful Augmentations	66.08	-7.99

augmentation methods are inferior than the simple ones, *e.g.*, RandomErasing and CutMix. When combing all positive augmentation methods, the REC performance encounters a significant decline, as shown in Tab. II, which is opposite to that in object detection [66]. These results greatly differ REC from object detection in terms of data augmentation.

What are less important in one-stage REC? Compared with the above mentioned factors, the other components have less

impact on one-stage REC. Above all, the role of language encoder is not as important as that in other V&L tasks. By deploying the advanced designs like self-attention [51] and BERT embedding [52], the performance gains are not obvious. Even on RefCOCOg, of which expressions are long and complex, the improvement is only +1.53%. One assumption about this result is that the expressions of REC is not so difficult to understand. But more importantly, it may also suggest that REC is less affected by language priors, which is often serious in other V&L tasks [31], [32], [68]. In this case, a simple design can meet the requirement of expression comprehension.

In Tab. I, we evaluate the effects of different loss functions and training tricks. The loss functions are deployed on the anchor-based detector [46], while their performance gains are not obvious, especially compared with object detection [54]. This results may suggest that pre-defined anchors are not

²Inference speed is tested on the 1080 Ti.

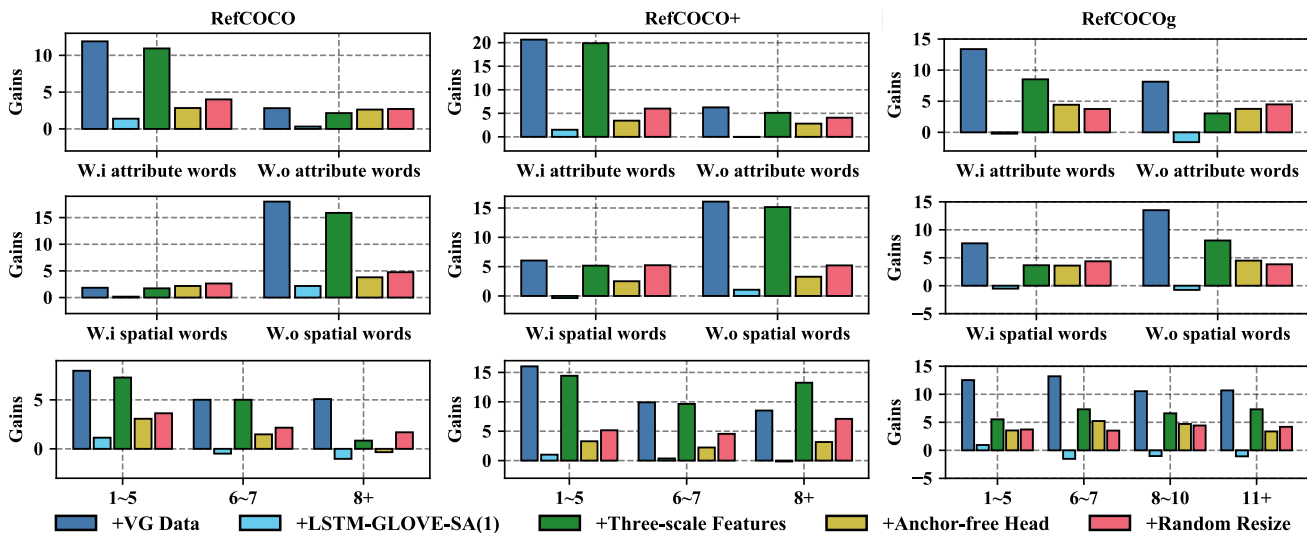


Fig. 4: Relative performance gains of five settings in SimREC on attribute descriptions (row-1), spatial descriptions (row-2), the expression length (row-3). All results are calculated on the *val* set.

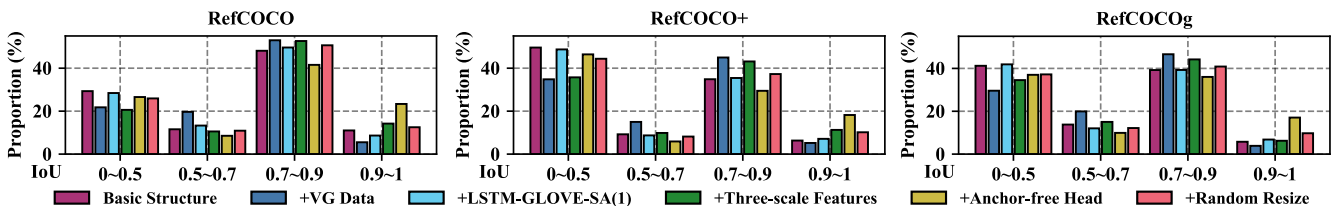


Fig. 5: Distribution of the predicted bounding boxes on different IoU metrics. All results are calculated on the *val* set.

TABLE III: Cumulative Ablations of SimREC on three REC datasets.

Models	Net #Params ³	RefCOCO				RefCOCO+			RefCOCOg		Inference Speed ²									
		val	testA	testB	val	testA	testB	val	test											
Basic Structure	7M	70.63	+0.00	72.28	+0.00	66.50	+0.00	50.39	+0.00	52.93	+0.00	45.12	+0.00	58.78	+0.00	58.58	+0.00	58.8	fps	+0.0
+ Three-scale Features	12M	77.41	+6.78	81.14	+8.86	71.85	+5.35	64.72	+14.33	69.09	+16.16	59.49	+14.37	65.51	+6.73	64.82	+6.24	50.0	fps	-8.8
+ LSTM-GLOVE-SA(1)	16M	78.21	+7.58	81.22	+8.94	71.94	+5.44	64.83	+14.44	70.22	+17.29	55.23	+10.11	66.65	+7.87	66.57	+7.99	48.8	fps	-10.0
+ Anchor-free Head	16M	79.74	+9.11	82.67	+10.39	73.56	+7.06	68.25	+17.86	73.12	+20.19	58.45	+13.33	69.22	+10.44	69.18	+10.60	47.9	fps	-10.9
+ Optimizations	16M	80.88	+10.25	83.23	+10.95	75.22	+8.72	68.57	+18.18	73.65	+20.72	58.79	+13.67	69.26	+10.48	69.45	+10.87	47.9	fps	-10.9
+ Random Resize	16M	82.03	+11.40	85.01	+12.73	77.65	+11.15	70.24	+19.85	75.87	+22.94	60.87	+15.75	71.43	+12.65	71.21	+12.63	47.9	fps	-10.9
+ CSPDarknet	16M	82.45	+11.82	85.91	+13.63	77.98	+11.48	70.58	+20.19	76.75	+23.82	61.12	+16.00	72.59	+13.81	72.86	+14.28	55.6	fps	-3.2
+ VG Data	16M	86.49	+15.86	88.95	+16.67	81.74	+15.24	77.51	+27.12	82.68	29.75	68.81	+23.69	79.88	+21.10	79.56	+20.98	55.6	fps	-3.2

suitable for one-stage REC. In terms of model optimization, all candidate methods pose positive impacts on performance although not so obvious. Particularly, we find that EMA [58] can accelerate training convergence.

How do these factors affect REC? Based on the above findings, we further explore how these key factors affect one-stage REC. Specifically, we investigate their effects on expressions of different content and lengths in Fig. 4, and the quality of predicted bounding boxes in Fig. 5.

From Fig. 4, we can first observe that multi-scale features and data augmentations can improve the model performance on all expressions, especially the ones with attribute descriptions (words). In this regard, we think that multi-scale features are to enhance the visual representations to facilitate fine-grained recognition, while data augmentation can significantly strengthen the learning of language-vision alignments. These two aspects are critical for REC. In addition, we also notice

that the improvement of the expressions with spatial information (words) is small. We attribute it to the intrinsic merit of one-stage REC modeling in spatial relation modeling [1]. Meanwhile, we can also find that with the improvement in visual modeling, the model also has a better ability to process the long and complex expressions, especially with the help of VG. This result also provides a useful hint for the study of multi-modal reasoning.

Compared with these two factors, the benefit of detection head is more balanced. For this end, we understand that detection head mainly affects the model’s detection ability. Besides, Fig. 4 also reflects the inference of language encoder, which is relatively small. Since most of the sentences in benchmark datasets are short, the help of language encoder is not obvious. In contrast, it also affects its performance on long sentences. This observation is consistent with the experimental results in Tab. I.

TABLE IV: Comparison of SimREC and the state-of-the-arts on three REC datasets. SimREC (scratch) is not pre-trained on VG.

Models	Visual Features	Net #Params ³	RefCOCO			RefCOCO+			RefCOCog		Inference Speed ²
			val	testA	testB	val	testA	testB	val-u	test-u	
<i>Two-stage:</i>											
CMN [33] _{CVPR17}	VGG16	-	-	71.03	65.77	-	54.32	47.76	-	-	-
MAttNet [3] _{CVPR18}	RN101	18M	76.65	81.14	69.99	65.33	71.62	56.02	66.58	67.27	2.6 fps
NMTree [6] _{JCCV19}	RN101	-	76.41	81.21	70.09	66.46	72.02	57.52	65.87	66.44	-
CM-Att-Erase [17] _{CVPR19}	RN101	-	78.35	83.14	71.32	68.09	73.65	58.03	67.99	68.67	-
<i>One-stage:</i>											
RealGIN [1] _{TNNLS21}	DN53	12M	77.25	78.70	72.10	62.78	67.17	54.21	62.75	62.33	52.6 fps
FAOA* [7] _{ICCV19}	DN53	120M	72.54	74.35	68.50	56.81	60.23	49.60	61.33	60.36	25.0 fps
ReSC* [8]	DN53	120M	77.63	80.45	72.30	63.59	68.36	56.81	67.30	67.20	18.9 fps
MCN [2] _{CVPR20}	DN53	26M	80.08	82.29	74.98	67.16	72.86	57.31	66.46	66.01	19.6 fps
Iter-Shrinking [4] _{CVPR21}	RN101	-	-	74.27	68.10	-	71.05	58.25	-	<u>70.05</u>	-
LBYL-Net* [18] _{CVPR21}	DN53	115M	79.67	82.91	74.15	68.64	73.38	59.49	-	-	27.0 fps
TransVG [9] _{ICCV21}	RN101	117M	<u>81.02</u>	<u>82.72</u>	<u>78.35</u>	64.82	70.70	56.94	<u>68.67</u>	67.73	19.6 fps
SimREC (scratch)	DN53	16M	82.03	85.01	77.65	70.24	75.39	61.85	71.43	72.07	50.0 fps
SimREC (scratch)	CDN53	16M	82.45	85.91	77.98	70.58	76.75	61.12	72.59	72.86	55.6 fps
SimREC	CDN53	16M	86.49	88.95	81.74	77.51	82.68	68.81	79.88	79.56	55.6 fps

* denotes the visual backbone is pre-trained on the whole MS-COCO *train* set.

TABLE V: Comparison of SimREC and pre-trained models on three REC datasets. † denotes that we use the same number of images as MDETR to pre-train SimREC.

Models	Visual Features	Pretrain Images	Net #Params ³	RefCOCO			RefCOCO+			RefCOCog		Inference Speed ²
				val	testA	testB	val	testA	testB	val-u	test-u	
VilBERT [16] _{NeurIPS19}	RN101	3.3M	221M	-	-	-	72.34	78.52	62.61	-	-	2.5 fps
ERNIE-ViL-L [22] _{AAAI21}	RN101	4.3M	-	-	-	-	75.89	82.37	66.91	-	-	-
UNITER-L [20] _{ECCV20}	RN101	4.6M	335M	81.41	87.04	74.17	75.90	81.45	66.70	74.86	75.77	2.4 fps
VILLA-L [21] _{NeurIPS20}	RN101	4.6M	335M	82.39	87.48	74.84	76.17	81.54	66.84	76.18	76.71	2.4 fps
MDETR [44] _{ICCV21}	RN101	0.2M	143M	86.75	89.58	81.41	<u>79.52</u>	<u>84.09</u>	<u>70.62</u>	<u>81.64</u>	<u>80.89</u>	15.4 fps
SimREC	DN53	0.1M	16M	85.72	88.10	81.28	76.11	81.57	66.49	77.78	78.28	50.0 fps
SimREC	CDN53	0.1M	16M	86.49	88.95	81.74	77.51	82.68	68.81	79.88	79.56	55.6 fps
SimREC	CDN53	0.2M†	16M	88.47	90.75	84.10	80.25	85.33	72.04	83.08	83.99	55.6 fps

TABLE VI: Comparison of SimREC and the state-of-the-arts on Referit and Flickr.

Models	Visual Features	Referit test	Flickr test
<i>Two-stage:</i>			
MAttNet [3]	RN101	29.04	-
Similarity Net [60]	RN101	34.54	60.89
DDPN [61]	RN101	63.00	73.30
<i>One-stage:</i>			
ZSGNet [15]	RN50	58.63	63.39
FAOA [7]	DN53	60.67	68.71
ReSC [8]	DN53	64.60	69.28
TransVG [9]	RN101	<u>70.73</u>	<u>79.10</u>
SimREC	CDN53	77.80	83.31

Fig. 5 depicts the IoU score distributions of the model’s predictions about the ground-truth bounding boxes. These results reflect the impact of these factors on the quality of model predictions. From this figure, we observe that the anchor-free detector obviously improves the detection ability. On the high-quality detection (IoU 0.9-1), the number is almost doubled by this detector. Meanwhile, we notice that the use of VG helps the model improve the detection accuracy (IoU>0.5), but its performance on high-quality detection declines obviously. This is mainly attributed to the less accurate bounding box annotations in VG [28].

³The calculation of network parameters excludes the visual backbone.

2) *Comparison with the state-of-the-art methods.*: After making trade-offs between performance and efficiency, we further combine some findings from Tab. III to strengthen our baseline network SimREC. The cumulative ablation results are given in Tab. III. Then, we compare SimREC to a set of state-of-the-art (SOTA) methods in REC.

Comparison to one-stage and two-stage SOTAs. We first compare SimREC with the SOTA methods specifically designed for REC, of which results are given in Tab. IV and Tab. VI. From this table, we can see that SimREC outperforms all these methods by a large margin, *e.g.*, +6.23%, +9.23% and +11.21% on three datasets, respectively. Even without using VG as additional data, the performance gains of SimREC are still obvious, *e.g.*, +up to 3.37% on RefCOCO+. Besides, SimREC also have superior efficiency. With much better performance, SimREC further enhances the speed advantage against two-stage methods, *e.g.*, +21.4 times. Compared with one-stage SOTAs, it is also faster, *i.e.*, +3.0 FPS.

Comparison with large-scale pre-trained models. We also compare SimREC with a set of large-scale pre-trained models in Tab. V, which includes ViLBert [16], ERNIE-ViL [22], UNITER [20] and VILLA [21]. These methods all apply the expensive BERT-style pre-training with millions of vision-language examples [13], [28], [69], [70], and they are also fine-tuned on REC datasets. From Tab. V, we surprisingly observe that our simple yet lightweight model can outperform these

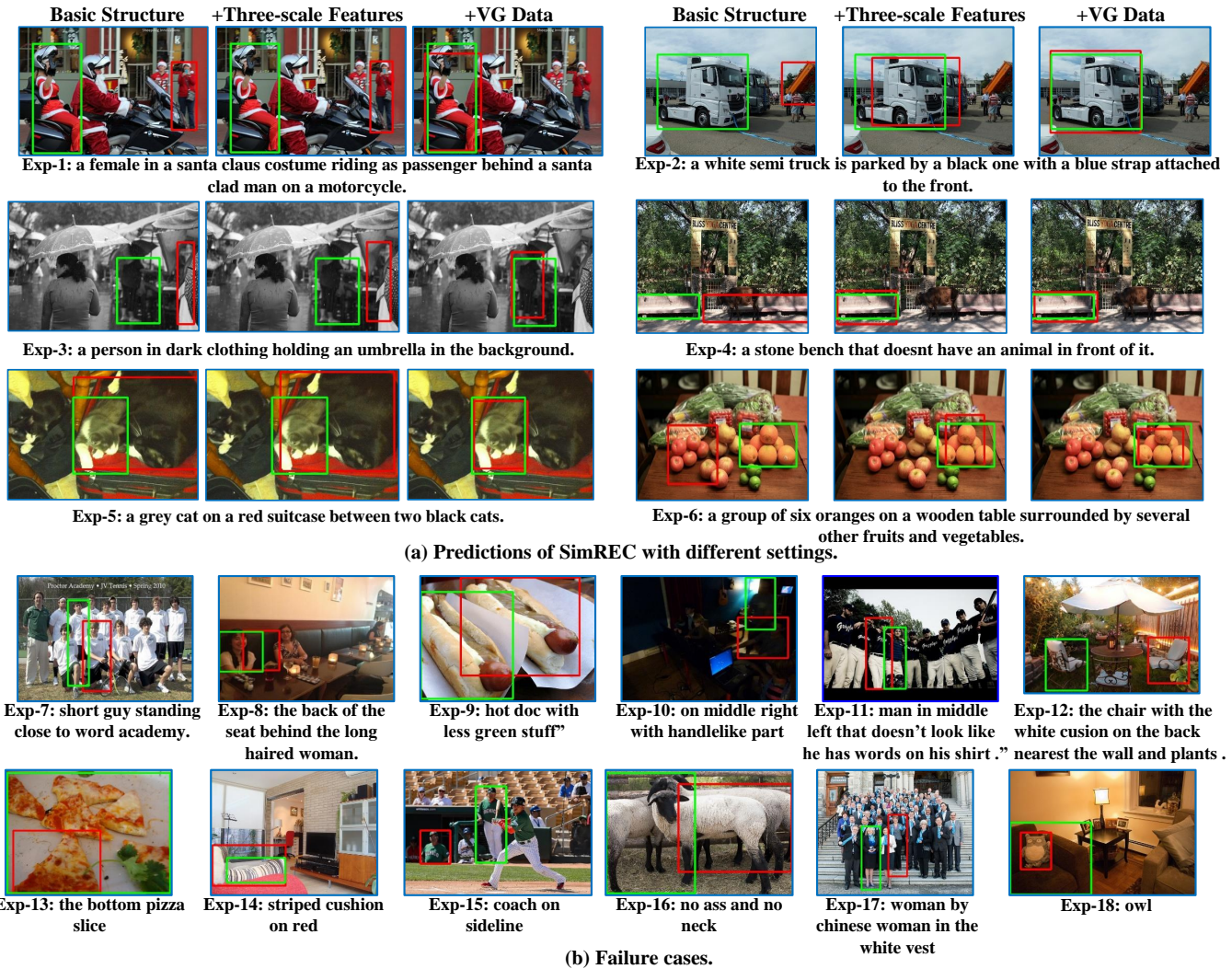


Fig. 6: Visualizations of predictions by SimREC with different settings and failure cases. The box of green color is the ground-truth, and the one of red is the prediction.

large models on all benchmark datasets. On RefCOCO *testB*, the performance gains can be up to +6.9%. Meanwhile, we compare SimREC with recent MDETR [44], which also uses extra REC data to pre-train the model. Compared to MDETR, SimREC also performs better in terms of performance and speed. More importantly, the parameter size and training overhead of SimREC are all far less than these methods. Since these large models have dominated various V&L tasks [13], [32], this result is much beyond expectations.

3) *Qualitative Analysis.*: In Fig. 6, we visualize the predictions by SimREC with different settings, and also give some typical failure cases.

From Fig. 6(a), we can observe that without multi-scale features and data augmentation, SimREC is easy to fail to understand the expression containing various attributes or relationships. The adoption of multi-scale features and data augmentation can obviously help the model in visual concept understanding as well as relational reasoning. Fig. 6(b) lists the common failure detections in the well-improved SimREC. Some of them are attributed to the label noisy, *e.g.*, the 7-*th* and 8-*th* examples, while some are too abstract or beyond the

ability of REC. For instance, the 1-*st* example requires the model to understand the characters in the image. However, these failure cases cannot conceal the outstanding ability of SimREC after adopting our findings.

V. CONCLUSION

In this paper, we present an empirical study for one-stage REC, which ablates 42 candidate designs/settings via over 100 experimental trails. This study not only yields the key factors for one-stage REC in addition to multi-modal fusion, but also reflects some findings against common impressions about REC. By combing the empirical findings, we also improve the simple REC network (SimREC) by a large margin, which greatly outperforms existing REC models in both accuracy and efficiency. More importantly, SimREC have better performance than a set of large-scale pre-trained V&L models with much less training overhead and parameters. We believe that the findings of this paper can provide useful references for the development of REC, and also give some inspirations for the V&L research.

ACKNOWLEDGMENT

This work is supported by the National Science Fund for Distinguished Young Scholars (No.62025603), the National Natural Science Foundation of China (No.U1705262, No. 62072386, No. 62072387, No. 62072389, No.62002305, No.61772443, No.61802324 and No.61702136), Guangdong Basic and Applied Basic Research Foundation (No.2019B1515120049), the Natural Science Foundation of Fujian Province of China (No.2021J01002), and the Fundamental Research Funds for the central universities (No. 20720200077, No. 20720200090 and No. 20720200091).

REFERENCES

- [1] Y. Zhou, R. Ji, G. Luo, X. Sun, J. Su, X. Ding, C.-W. Lin, and Q. Tian, "A real-time global inference network for one-stage referring expression comprehension," *IEEE Transactions on Neural Networks and Learning Systems*, 2021.
- [2] G. Luo, Y. Zhou, X. Sun, L. Cao, C. Wu, C. Deng, and R. Ji, "Multi-task collaborative network for joint referring expression comprehension and segmentation," in *Proceedings of the IEEE/CVF Conference on Computer Vision and Pattern Recognition*, 2020, pp. 10034–10043.
- [3] L. Yu, Z. Lin, X. Shen, J. Yang, X. Lu, M. Bansal, and T. L. Berg, "M attnet: Modular attention network for referring expression comprehension," in *CVPR*, 2018.
- [4] M. Sun, J. Xiao, and E. G. Lim, "Iterative shrinking for referring expression grounding using deep reinforcement learning," in *Proceedings of the IEEE/CVF Conference on Computer Vision and Pattern Recognition*, 2021, pp. 14 060–14 069.
- [5] P. Wang, Q. Wu, J. Cao, C. Shen, L. Gao, and A. v. d. Hengel, "Neighbourhood watch: Referring expression comprehension via language-guided graph attention networks," in *CVPR*, 2019.
- [6] D. Liu, H. Zhang, F. Wu, and Z.-J. Zha, "Learning to assemble neural module tree networks for visual grounding," in *ICCV*, 2019.
- [7] Z. Yang, B. Gong, L. Wang, W. Huang, D. Yu, and J. Luo, "A fast and accurate one-stage approach to visual grounding," in *ICCV*, 2019.
- [8] Z. Yang, T. Chen, L. Wang, and J. Luo, "Improving one-stage visual grounding by recursive sub-query construction," *arXiv preprint arXiv:2008.01059*, 2020.
- [9] J. Deng, Z. Yang, T. Chen, W. Zhou, and H. Li, "Transvg: End-to-end visual grounding with transformers," *arXiv preprint arXiv:2104.08541*, 2021.
- [10] M. Bajaj, L. Wang, and L. Sigal, "G3rground: Graph-based language grounding," in *Proceedings of the IEEE/CVF International Conference on Computer Vision*, 2019, pp. 4281–4290.
- [11] P. Dogan, L. Sigal, and M. Gross, "Neural sequential phrase grounding (seqground)," in *Proceedings of the IEEE/CVF Conference on Computer Vision and Pattern Recognition*, 2019, pp. 4175–4184.
- [12] K. Chen, R. Kovvuri, and R. Nevatia, "Query-guided regression network with context policy for phrase grounding," in *Proceedings of the IEEE International Conference on Computer Vision*, 2017, pp. 824–832.
- [13] T. Lin, M. Maire, S. J. Belongie, J. Hays, P. Perona, D. Ramanan, P. Dollar, and C. L. Zitnick, "Microsoft coco: Common objects in context," in *ECCV*, 2014.
- [14] S. Shao, Z. Li, T. Zhang, C. Peng, G. Yu, X. Zhang, J. Li, and J. Sun, "Objects365: A large-scale, high-quality dataset for object detection," in *Proceedings of the IEEE/CVF International Conference on Computer Vision*, 2019, pp. 8430–8439.
- [15] A. Sadhu, K. Chen, and R. Nevatia, "Zero-shot grounding of objects from natural language queries," in *ICCV*, 2019.
- [16] J. Lu, D. Batra, D. Parikh, and S. Lee, "Vilbert: Pretraining task-agnostic visiolinguistic representations for vision-and-language tasks," *arXiv preprint arXiv:1908.02265*, 2019.
- [17] X. Liu, Z. Wang, J. Shao, X. Wang, and H. Li, "Improving referring expression grounding with cross-modal attention-guided erasing," in *Proceedings of the IEEE/CVF Conference on Computer Vision and Pattern Recognition*, 2019, pp. 1950–1959.
- [18] B. Huang, D. Lian, W. Luo, and S. Gao, "Look before you leap: Learning landmark features for one-stage visual grounding," in *Proceedings of the IEEE/CVF Conference on Computer Vision and Pattern Recognition*, 2021, pp. 16 888–16 897.
- [19] L. Yu, P. Poirson, S. Yang, A. C. Berg, and T. L. Berg, "Modeling context in referring expressions," in *European Conference on Computer Vision*. Springer, 2016, pp. 69–85.
- [20] Y.-C. Chen, L. Li, L. Yu, A. El Kholy, F. Ahmed, Z. Gan, Y. Cheng, and J. Liu, "Uniter: Universal image-text representation learning," in *European conference on computer vision*. Springer, 2020, pp. 104–120.
- [21] Z. Gan, Y.-C. Chen, L. Li, C. Zhu, Y. Cheng, and J. Liu, "Large-scale adversarial training for vision-and-language representation learning," in *NeurIPS*, 2020.
- [22] F. Yu, J. Tang, W. Yin, Y. Sun, H. Tian, H. Wu, and H. Wang, "Ernie-vil: Knowledge enhanced vision-language representations through scene graphs," in *Proceedings of the AAAI Conference on Artificial Intelligence*, vol. 35, no. 4, 2021, pp. 3208–3216.
- [23] V. K. Nagaraja, V. I. Morariu, and L. S. Davis, "Modeling context between objects for referring expression understanding," in *ECCV*, 2016.
- [24] Z. Zhong, L. Zheng, G. Kang, S. Li, and Y. Yang, "Random erasing data augmentation," in *Proceedings of the AAAI Conference on Artificial Intelligence*, vol. 34, no. 07, 2020, pp. 13 001–13 008.
- [25] E. D. Cubuk, B. Zoph, J. Shlens, and Q. V. Le, "Randaugment: Practical automated data augmentation with a reduced search space," in *Proceedings of the IEEE/CVF Conference on Computer Vision and Pattern Recognition Workshops*, 2020, pp. 702–703.
- [26] S. Yun, D. Han, S. J. Oh, S. Chun, J. Choe, and Y. Yoo, "Cutmix: Regularization strategy to train strong classifiers with localizable features," in *Proceedings of the IEEE/CVF International Conference on Computer Vision*, 2019, pp. 6023–6032.
- [27] T. DeVries and G. W. Taylor, "Improved regularization of convolutional neural networks with cutout," *arXiv preprint arXiv:1708.04552*, 2017.
- [28] R. Krishna, Y. Zhu, O. Groth, J. Johnson, K. Hata, J. Kravitz, S. Chen, Y. Kalantidis, L.-J. Li, D. A. Shamma *et al.*, "Visual genome: Connecting language and vision using crowdsourced dense image annotations," in *arXiv preprint*, 2016.
- [29] Z. Yu, J. Yu, Y. Cui, D. Tao, and Q. Tian, "Deep modular co-attention networks for visual question answering," in *Proceedings of the IEEE/CVF Conference on Computer Vision and Pattern Recognition*, 2019, pp. 6281–6290.
- [30] D.-K. Nguyen, V. Goswami, and X. Chen, "Revisiting modulated convolutions for visual counting and beyond," *arXiv preprint arXiv:2004.11883*, 2020.
- [31] S. Antol, A. Agrawal, J. Lu, M. Mitchell, D. Batra, C. L. Zitnick, and D. Parikh, "Vqa: Visual question answering," in *ICCV*, 2015.
- [32] H. Xu and K. Saenko, "Ask, attend and answer: Exploring question-guided spatial attention for visual question answering," in *ECCV*, 2016.
- [33] R. Hu, M. Rohrbach, J. Andreas, T. Darrell, and K. Saenko, "Modeling relationships in referential expressions with compositional modular networks," in *CVPR*, 2017.
- [34] R. Hu, H. Xu, M. Rohrbach, J. Feng, K. Saenko, and T. Darrell, "Natural language object retrieval," in *CVPR*, 2016.
- [35] J. Liu, L. Wang, and M. Yang, "Referring expression generation and comprehension via attributes," in *ICCV*, 2017.
- [36] R. Luo and G. Shakhnarovich, "Comprehension-guided referring expressions," in *CVPR*, 2017.
- [37] L. Yu, P. Poirson, S. Yang, A. C. Berg, and T. L. Berg, "Modeling context in referring expressions," in *ECCV*, 2016.
- [38] L. Yu, H. Tan, M. Bansal, and T. L. Berg, "A joint speaker-listener-reinforcer model for referring expressions," in *CVPR*, 2017.
- [39] Y. Zhang, L. Yuan, Y. Guo, Z. He, I. Huang, and H. Lee, "Discriminative bimodal networks for visual localization and detection with natural language queries," in *CVPR*, 2017.
- [40] L. Yu, Z. Lin, X. Shen, J. Yang, X. Lu, M. Bansal, and T. L. Berg, "M attnet: Modular attention network for referring expression comprehension," in *CVPR*, 2018.
- [41] Y. Zhou, T. Ren, C. Zhu, X. Sun, J. Liu, X. Ding, M. Xu, and R. Ji, "Trar: Routing the attention spans in transformer for visual question answering," in *Proceedings of the IEEE/CVF International Conference on Computer Vision*, 2021, pp. 2074–2084.
- [42] S. Ren, K. He, R. Girshick, and J. Sun, "Faster r-cnn: towards real-time object detection with region proposal networks," in *TPAMI*, 2017.
- [43] A. Sadhu, K. Chen, and R. Nevatia, "Zero-shot grounding of objects from natural language queries," in *Proceedings of the IEEE/CVF International Conference on Computer Vision*, 2019, pp. 4694–4703.
- [44] A. Kamath, M. Singh, Y. LeCun, G. Synnaeve, I. Misra, and N. Carion, "M detr-modulated detection for end-to-end multi-modal understanding," in *Proceedings of the IEEE/CVF International Conference on Computer Vision*, 2021, pp. 1780–1790.

- [45] V. Nair and G. E. Hinton, "Rectified linear units improve restricted boltzmann machines," in *Icml*, 2010.
- [46] J. Redmon and A. Farhadi, "Yolov3: An incremental improvement," in *arXiv preprint*, 2018.
- [47] K. Simonyan and A. Zisserman, "Very deep convolutional networks for large-scale image recognition," in *ICLR*, 2015.
- [48] C.-Y. Wang, H.-Y. M. Liao, Y.-H. Wu, P.-Y. Chen, J.-W. Hsieh, and I.-H. Yeh, "Cspnet: A new backbone that can enhance learning capability of cnn," in *Proceedings of the IEEE/CVF conference on computer vision and pattern recognition workshops*, 2020, pp. 390–391.
- [49] S. Hochreiter and J. Schmidhuber, "Long short-term memory," in *Neural computation*, 1997.
- [50] J. Pennington, R. Socher, and C. Manning, "Glove: Global vectors for word representation," in *EMNLP*, 2014.
- [51] A. Vaswani, N. Shazeer, N. Parmar, J. Uszkoreit, L. Jones, A. N. Gomez, L. Kaiser, and I. Polosukhin, "Attention is all you need," in *NIPS*, 2017.
- [52] J. Devlin, M. Chang, K. Lee, and K. Toutanova, "Bert: Pre-training of deep bidirectional transformers for language understanding," in *arXiv preprint*, 2018.
- [53] Z. Ge, S. Liu, F. Wang, Z. Li, and J. Sun, "Yolox: Exceeding yolo series in 2021," *arXiv preprint arXiv:2107.08430*, 2021.
- [54] H. Rezaatofghi, N. Tsoi, J. Gwak, A. Sadeghian, I. Reid, and S. Savarese, "Generalized intersection over union: A metric and a loss for bounding box regression," in *Proceedings of the IEEE/CVF Conference on Computer Vision and Pattern Recognition*, 2019, pp. 658–666.
- [55] T.-Y. Lin, P. Goyal, R. Girshick, K. He, and P. Dollár, "Focal loss for dense object detection," in *Proceedings of the IEEE international conference on computer vision*, 2017, pp. 2980–2988.
- [56] H. Zhang, M. Cisse, Y. N. Dauphin, and D. Lopez-Paz, "mixup: Beyond empirical risk minimization," *arXiv preprint arXiv:1710.09412*, 2017.
- [57] T. He, Z. Zhang, H. Zhang, Z. Zhang, J. Xie, and M. Li, "Bag of tricks for image classification with convolutional neural networks," in *Proceedings of the IEEE/CVF Conference on Computer Vision and Pattern Recognition*, 2019, pp. 558–567.
- [58] A. Tarvainen and H. Valpola, "Mean teachers are better role models: Weight-averaged consistency targets improve semi-supervised deep learning results," *arXiv preprint arXiv:1703.01780*, 2017.
- [59] J. Mao, J. Huang, A. Toshev, O. M. Camburu, A. L. Yuille, and K. P. Murphy, "Generation and comprehension of unambiguous object descriptions," in *CVPR*, 2016.
- [60] L. Wang, Y. Li, J. Huang, and S. Lazebnik, "Learning two-branch neural networks for image-text matching tasks," *IEEE Transactions on Pattern Analysis and Machine Intelligence*, vol. 41, no. 2, pp. 394–407, 2018.
- [61] Z. Yu, J. Yu, C. Xiang, Z. Zhao, Q. Tian, and D. Tao, "Rethinking diversified and discriminative proposal generation for visual grounding," *arXiv preprint arXiv:1805.03508*, 2018.
- [62] J. C. Duchi, E. Hazan, and Y. Singer, "Adaptive subgradient methods for online learning and stochastic optimization," in *JMLR*, 2011.
- [63] R. Krishna, Y. Zhu, O. Groth, J. Johnson, K. Hata, J. Kravitz, S. Chen, Y. Kalantidis, L.-J. Li, D. A. Shamma *et al.*, "Visual genome: Connecting language and vision using crowdsourced dense image annotations," *International journal of computer vision*, vol. 123, no. 1, pp. 32–73, 2017.
- [64] H. Jiang, I. Misra, M. Rohrbach, E. Learned-Miller, and X. Chen, "In defense of grid features for visual question answering," in *Proceedings of the IEEE/CVF Conference on Computer Vision and Pattern Recognition*, 2020, pp. 10267–10276.
- [65] G. Luo, Y. Zhou, R. Ji, X. Sun, J. Su, C.-W. Lin, and Q. Tian, "Cascade grouped attention network for referring expression segmentation," in *Proceedings of the 28th ACM International Conference on Multimedia*, 2020, pp. 1274–1282.
- [66] Z. Zhang, T. He, H. Zhang, Z. Zhang, J. Xie, and M. Li, "Bag of freebies for training object detection neural networks," *arXiv preprint arXiv:1902.04103*, 2019.
- [67] P. Anderson, X. He, C. Buehler, D. Teney, M. Johnson, S. Gould, and L. Zhang, "Bottom-up and top-down attention for image captioning and visual question answering," in *CVPR*, 2018.
- [68] R. Kiros, R. Salakhutdinov, and R. S. Zemel, "Multimodal neural language models," in *ICML*, 2014.
- [69] P. Sharma, N. Ding, S. Goodman, and R. Soicrut, "Conceptual captions: A cleaned, hypernymed, image alt-text dataset for automatic image captioning," in *Proceedings of the 56th Annual Meeting of the Association for Computational Linguistics (Volume 1: Long Papers)*, 2018, pp. 2556–2565.
- [70] V. Ordonez, G. Kulkarni, and T. Berg, "Im2text: Describing images using 1 million captioned photographs," *Advances in neural information processing systems*, vol. 24, pp. 1143–1151, 2011.



Gen Luo is currently pursuing the phd's degree in Xiamen University. His research interests include vision-and-language interactions.



Yiyi Zhou received his Ph.D. degree supervised by Prof. Rongrong Ji from Xiamen University, China, in 2019. He is a Post-doctoral Research Fellow of the School of Informatics and a member of Media Analytics and Computing (MAC) lab of Xiamen University, China.



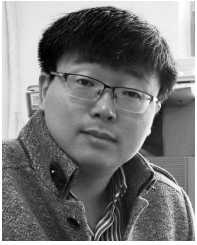
Jiamu Sun received his Bachelor Degree from Hebei University of Technology, China, in 2021. He is a postgraduate student supervised by Prof. Rongrong Ji in Media Analytics and Computing (MAC) lab of Xiamen University, China.



Shubin Huang received his bachelor's degree from FuZhou University, China, in 2021. He is a post-graduate of the School of Informatics and a member of Media Analytics and Computing (MAC) lab of Xiamen University, China.



Xiaoshuai Sun (Senior Member, IEEE) received the B.S. degree in computer science from Harbin Engineering University, Harbin, China, in 2007, and the M.S. and Ph.D. degrees in computer science and technology from the Harbin Institute of Technology, Harbin, in 2009 and 2015, respectively. He was a Postdoctoral Research Fellow with the University of Queensland from 2015 to 2016. He served as a Lecturer with the Harbin Institute of Technology from 2016 to 2018. He is currently an Associate Professor with Xiamen University, China. He was a recipient of the Microsoft Research Asia Fellowship in 2011.



Qixiang Ye received the B.S. and M.S. degrees in mechanical and electrical engineering from the Harbin Institute of Technology, China, in 1999 and 2001, respectively, and the Ph.D. degree from the Institute of Computing Technology, Chinese Academy of Sciences, China, in 2006. He was a Visiting Assistant Professor with the Institute of Advanced Computer Studies (UMIACS), University of Maryland, College Park, Maryland, in 2013, and a Visiting Scholar with IIID, Duke University, Durham, NC, USA, in 2016. Since 2016, he has been a Professor

with the University of Chinese Academy of Sciences, China. He has published more than 100 papers in refereed conferences and journals, including the IEEE CVPR, ICCV, ECCV, the *IEEE Transactions on Intelligent Transportation Systems*, the *IEEE Transactions on Image Processing*, and the *IEEE Transactions on Pattern Analysis and Machine Intelligence*. His research interests include image processing, visual object detection, and machine learning. He received the Sony Outstanding Paper Award.



Yongjian Wu received his master's degree in computer science from Wuhan University, China, in 2008. He is currently the expert researcher and the director of the YouTu Lab, Tencent Co., Ltd. His research interests include face recognition, image understanding, and large scale data processing.



Rongrong Ji (Senior Member, IEEE) is a Nanqiang Distinguished Professor at Xiamen University, the Deputy Director of the Office of Science and Technology at Xiamen University, and the Director of Media Analytics and Computing Lab. He was awarded as the National Science Foundation for Excellent Young Scholars (2014), the National Ten Thousand Plan for Young Top Talents (2017), and the National Science Foundation for Distinguished Young Scholars (2020). His research falls in the field of computer vision, multimedia analysis, and

machine learning. He has published 50+ papers in ACM/IEEE Transactions, including TPAMI and IJCV, and 100+ full papers on top-tier conferences, such as CVPR and NeurIPS. His publications have got over 10K citations in Google Scholar. He was the recipient of the Best Paper Award of ACM Multimedia 2011. He has served as Area Chairs in top-tier conferences such as CVPR and ACM Multimedia. He is also an Advisory Member for Artificial Intelligence Construction in the Electronic Information Education Committee of the National Ministry of Education.